Numerical Methods in Civil Engineering, 6-4 (2022) 38-46

Numerical Methods in Civil Engineering

Journal Homepage: https://nmce.kntu.ac.ir/

On the response spectra of cracked beams under different types of moving force

Saharnaz Zalaghi * and Ali Nikkhoo **

ARTICLE INFO

RESEARCH PAPER

Article history:
Received:
August 2021.
Revised:
December 2021.
Accepted:
January 2022.

Keywords:
Euler-Bernoulli beam,
Cracked beam,
Moving load,
Moving mass,
Moving oscillator,
Moving system,
Response spectra.

Abstract:

In this paper, the dynamic responses of cracked beams under different moving forces, including moving load, moving mass, moving oscillator, and four-degrees-of-freedom moving system, are investigated. Structural elements such as beams are designed to withstand the predicted loads, but unfortunately, they are always exposed to unpredictable damage such as cracks. Several factors may cause these damages, and the important thing is that their presence can affect the dynamic behavior of the beam or even endanger its reliability and durability in some cases. Therefore, this study considers an Euler-Bernoulli single-span beam with simple supports and a crack. First, with the help of the function expansion method and by employing MATLAB software, the dynamic time history responses of the beam at its midpoint under the influence of each type of moving force are extracted. Then, the changes in maximum displacement responses due to various parameters such as velocity, load magnitude, crack depth, and crack location are plotted in different spectra and compared with each other. The results show that the beam will have close results under all types of moving force (moving load, moving oscillator, and moving system) except moving mass. Obviously, this difference is due to the effect of inertia on the moving mass.

1. Introduction

Beams are among the structural elements widely used in engineering designs and can be subjected to frequent static and dynamic loads. The existence of damages such as cracks in a beam caused by various factors can directly affect its dynamic behavior and, in some cases, endanger its reliability and durability. Therefore, in recent decades, scientists have studied the effect of cracks in beams in their research [1-7]. Lee et al. [8] surveyed the dynamic response of a cracked beam under a moving load. Law and Zhu [9] also investigated the dynamic behavior of a reinforced concrete bridge. They modeled vehicles as moving masses and moving systems with four degrees of freedom. Mahmoud and Abou Zaid [10] studied crack effects on the dynamic response of a beam subjected to a moving mass by focusing on the simply supported Euler-Bernoulli beam.

Rofooei et al. [11] used the governing differential equation of motion for an Euler-Bernoulli beam under moving mass, considering the centripetal and Coriolis accelerations besides the vertical component one. Kiani et al. [12] carried out parametric studies on the vibration of multi-span viscoelastic Euler–Bernoulli beams traversed by a moving mass. They used a total moving least square method for spatial discretization of the problem's parameters. A number of other studies on this topic have also been done by Kiani et al. [13-16]. Thatoi et al. [17] used finite element analysis and experimental techniques to validate their proposed procedure. They observed significant changes in mode shape at the crack location and declared that the variation in dynamic characteristics of the cracked cantilever beam could be utilized for the early assessment of cracks. In another study, Pala and Reis [18] investigated the effects of inertial, centripetal, and Coriolis forces on the dynamic response of a hinge-supported beam with a single crack under moving mass. Jena and Parhi [19] surveyed the

* *Ph.D. Student, School of Civil Engineering, College of Engineering, University of Tehran, Tehran, Iran.*
** *Corresponding Author: Assoc. Professor, Faculty of Engineering, University of Science and Culture, Tehran, Iran, Email: nikkhoo@usc.ac.ir*

[DOR: 20.1001.1.23454296.2022.6.4.2.9]
[DOI: 10.52547/nmce.6.4.38]

[DOR: 20.1001.1.23454296.2022.6.4.2.9]

[DOI: 10.52547/nmce.6.4.38]

dynamic response of a cracked cantilever beam with the presence of multiple open cracks with different positions and depths under a moving mass that has numerous mass magnitudes and speeds. The results taken from the numerical formulation showed good agreement with those of laboratory tests. Cicirello [20] investigated the response of damaged Euler–Bernoulli beams with some unilateral cracks and subjected to one or more moving masses that always remain in contact with them. Al Rjoub et al. [21] obtained an analytical solution using a modal expansion method to study the forced vibration response of multi-cracked Euler-Bernoulli and Timoshenko beams, including shear deformation and rotary inertia, with different boundary conditions and two moving loads which travel with constant velocity. Nikkhoo and Sharifinejad [22] scrutinized the effect of parameters such as the magnitude and speed of the moving force (including moving load and moving mass), its inertial effects, and crack's depth on the dynamic behavior of a simply supported Euler-Bernoulli beam. Other research on this area had also already been done by Nikkhoo [23-26]. A review of the previous studies shows that the transfer matrix method has been used to model the crack in the beam many times [9,27,28]. In this method, the crack is modeled as a rotational spring, and the beam parts are connected by it. Attar [29] probed an analytical approach to investigating natural frequencies and mode shapes of an Euler-Bernoulli beam with several cracks and different forms of boundary conditions. He modeled the stepped cracked beam as a group of uniform sub-segments connected by massless rotational springs. Al Rjoub et al. [30] studied the free vibration of multi-cracked, axially loaded beams with different boundary conditions, such as clamped-clamped, hinged-hinged, clamped-hinged, and clamped-free. They modeled cracked beams as several beam segments connected by massless rotational springs with sectional flexibility.

The purpose of the present paper is to investigate the effect of the vehicle modeling method (moving load, moving mass, moving oscillator, and moving system) on the dynamic behavior of cracked beams. In previous studies, the vehicle was modeled by a moving load or a moving oscillator. So, by upgrading the modeling method, a moving system that is a more realistic model of a vehicle is used.

This study investigates the effect of parameters such as velocity and load magnitude, crack depth ratio, crack location in the beam span, and the distance between axes of the moving system. Also, the passing effect of different types of moving forces, including moving load, moving mass, moving oscillator, and four-degrees-of-freedom moving system with a constant speed on the maximum displacement response of the beam is compared and discussed. Hence, by considering an Euler-Bernoulli beam in which there is a crack, the time history response of the mid-span of the beam under each type of moving force (moving load, moving mass, moving oscillator, or moving system) is calculated. A massless rotational spring and the transfer matrix method are used to model the crack and to obtain the mode shapes of the cracked beam. In each case, the maximum displacement response extracted from the time history responses is plotted and compared in different spectra. The results show that except for the situation in which the moving mass passes over the beam, it has almost similar dynamic responses under the other loading conditions.

2. Dynamic behavior of cracked beam under the moving forces

In this section, the behavior of a uniform Euler-Bernoulli beam under a moving force is studied. To investigate the effect of the type of moving force on the results, the force is examined in four conditions (moving load, moving mass, moving oscillator, and moving system). In all cases, the speed of the moving force is constant when crossing over the beam, and the contact surface of the force and the beam is assumed to be without friction. In general, the motion equation of a uniform Euler-Bernoulli beam under a moving force is as follows [31]:

$$EI\frac{\partial^4 w}{\partial x^4}(x,t)+\rho A\frac{\partial^2 w}{\partial t^2}(x,t)=f(x,t) \tag{1}$$

In the above equation, A is the cross-section of the beam, and L, ρ, I, and E are beam length, material destiny, second moment of area, and modulus of elasticity, respectively. $f(x,t)$ is also introduced later in this section according to the type of force model. To solve the above differential equation, the answer in the modal space is considered as follows:

$$w(x,t)=\sum_{i=1}^{n}\varphi_i(x)u_i(t) \tag{2}$$

where $w(x,t)$ is beam displacement response; $\varphi_i(x)$ and $u_i(t)$ are mode shape and modal coordinates of the ith mode, respectively.

By substituting Eq. (2) into Eq. (1) and also considering the orthogonal nature of the modes, the differential equation of motion of the beam is generally obtained for the first i modes:

$$\boldsymbol{M}\ddot{\boldsymbol{X}}(t)+\boldsymbol{C}\dot{\boldsymbol{X}}(t)+\boldsymbol{K}\boldsymbol{X}(t)=\boldsymbol{F}(t) \tag{3}$$

In the above equation, the parameters $\boldsymbol{M}$, $\boldsymbol{C}$, $\boldsymbol{K}$, $\boldsymbol{X}(t)$, and $\boldsymbol{F}(t)$ for each case are presented as in the following [11]:

2.1. Moving load

In the first case, a moving load of size mg goes through the beam. In this case, $f(x,t)$ is considered in Eq. (1) as follows:

$$f(x,t) = mg\,\delta(x - vt) \quad (4)$$

where δ is a function of the Dirac delta, and the parameters of Eq. (3) are defined as follows:

$$[\boldsymbol{M}]_{ij} = \rho A \int_0^L \varphi_i(x)\varphi_j(x)dx$$

$$[\boldsymbol{C}]_{ij} = 0$$

$$[\boldsymbol{K}]_{ij} = EI \int_0^L \varphi_i''(x)\varphi_j''(x)dx$$

$$[\boldsymbol{F}]_i = mg\,\varphi_i(x_m)$$

$$\boldsymbol{X}(t) = [u_1(t) \quad u_2(t) \quad \dots \quad u_n(t)]^T \quad (5)$$

In the above equation, x_m is the position of the moving load measured from the left support.

2.2. Moving mass

In the second case, the moving force is considered as a moving mass with mass m. In this case, $f(x,t)$ is considered in Eq. (1) as follows:

$$f(x,t) = m(g - \ddot{w}(x,t))\,\delta(x - vt) \quad (6)$$

where δ is a function of the Dirac delta, and the parameters of Eq. (3) are defined as follows:

$$[\boldsymbol{M}]_{ij} = \rho A \int_0^L \varphi_i(x)\varphi_j(x)dx + m\varphi_i(x_m)\varphi_j(x_m)$$

$$[\boldsymbol{C}]_{ij} = 2mv\,\varphi_i(x_m)\varphi_{j,x}(x_m)$$

$$[\boldsymbol{K}]_{ij} = EI \int_0^L \varphi_i''(x)\varphi_j''(x)dx + mv^2\varphi_i(x_m)\varphi_{j,xx}(x_m)$$

$$[\boldsymbol{F}]_i = mg\,\varphi_i(x_m)$$

$$\boldsymbol{X}(t) = [u_1(t) \quad u_2(t) \quad \dots \quad u_n(t)]^T \quad (7)$$

As before, x_m is the position of the moving mass measured from the left support.

2.3. Moving oscillator

In this part, the moving force is considered as a moving oscillator with the parameters shown in Fig. 1-c. Therefore, $f(x,t)$ in Eq. (1) and also the differential equation governing the moving oscillator motion are obtained as follows:

$$f(x,t) = m_w(g - \ddot{y}_w(t))\,\delta(x - vt) \quad (8)$$

$$m_w\ddot{y}_w(t) + c_w(\dot{y}_w(t) - \dot{w}(x,t)) + k_w(y_w(t) - w(x,t)) = 0 \quad (9)$$

where δ is a function of the Dirac delta, and the parameters of Eq. (3) are defined as follows:

$$\boldsymbol{M} = \begin{bmatrix} \boldsymbol{M}_b & \boldsymbol{M}_n \\ 0 & m_w \end{bmatrix}$$

$$\boldsymbol{C} = \begin{bmatrix} 0 & 0 \\ \boldsymbol{C}_n & c_w \end{bmatrix}$$

$$\boldsymbol{K} = \begin{bmatrix} \boldsymbol{K}_b & 0 \\ \boldsymbol{K}_n & k_w \end{bmatrix}$$

$$\boldsymbol{F} = \begin{bmatrix} \boldsymbol{F}_b \\ 0 \end{bmatrix}$$

$$\boldsymbol{X}(t) = [u_1(t) \quad u_2(t) \quad \dots \quad u_n(t) \quad y_w(t)]^T \quad (10)$$

Non-zero sub-matrices in the above equations are calculated as follows:

$$[\boldsymbol{M}_b]_{ij} = \rho A \int_0^L \varphi_i(x)\varphi_j(x)dx$$

$$[\boldsymbol{M}_n]_i = m_w\varphi_i(vt)$$

$$[\boldsymbol{C}_n]_j = -c_w\varphi_j(vt)$$

$$[\boldsymbol{K}_b]_{ij} = EI \int_0^L \varphi_i''(x)\varphi_j''(x)dx$$

$$[\boldsymbol{K}_n]_j = -k_w\varphi_j(vt)$$

$$[\boldsymbol{F}_b]_j = m_w g\,\varphi_j(vt) \quad (11)$$

2.4. Moving system

In this case, the moving force is considered as a moving system (a vehicle with three degrees of transient freedom and one degree of rotational freedom) with the parameters shown in Fig. 1-d. Therefore, $f(x,t)$ in Eq. (1) and also the differential equation governing the moving system motion is obtained as follows:

$$f(x,t) = \left(k_{1s}(y_1 - w(x_1(t),t)) + \left(m_1 + \frac{b_2}{b_1+b_2}\right)g\right)\delta(x - x_1(t)) + \left(k_{2s}(y_2 - w(x_2(t),t)) + \left(m_2 + \frac{b_1}{b_1+b_2}\right)g\right)\delta(x - x_2(t)) \quad (12)$$

$$I_v\ddot{\theta} + c_1b_1(\dot{y}_v - \dot{y}_1 + b_1\dot{\theta}) + k_1b_1(y_v - y_1 + b_1\theta) + -c_2b_2(\dot{y}_v - \dot{y}_2 - b_2\dot{\theta}) - k_2b_2(y_v - y_2 - b_2\theta) = 0 \quad (13)$$

$$m_v\ddot{y}_v + c_1(\dot{y}_v - \dot{y}_1 + b_1\dot{\theta}) + k_1(y_v - y_1 + b_1\theta) + +c_2(\dot{y}_v - \dot{y}_2 - b_2\dot{\theta}) + k_2(y_v - y_2 - b_2\theta) = 0 \quad (14)$$

$$m_1\ddot{y}_1 - c_1(\dot{y}_v - \dot{y}_1 + b_1\dot{\theta}) - k_1(y_v - y_1 + b_1\theta) + +k_{1s}(y_1 - w(x_1(t),t)) = 0 \quad (15)$$

$$m_2\ddot{y}_2 - c_2(\dot{y}_v - \dot{y}_2 - b_2\dot{\theta}) - k_2(y_v - y_2 - b_2\theta) + +k_{2s}(y_2 - w(x_2(t),t)) = 0 \quad (16)$$

In the above relations, $x_1(t)$ and $x_2(t)$ show the position of the first and second wheels of the moving system on the beam, respectively, and are defined as follows:

$$x_1(t) = vt - (b_1 + b_2)$$

[DOR: 20.1001.1.23454296.2022.6.4.2.9]
[DOI: 10.52547/nmce.6.4.38]

$$x_2(t) = vt \tag{17}$$

In this case, the parameters of Eq. (3) are defined as follows:

$$\boldsymbol{M} = \begin{bmatrix} \boldsymbol{M}_b & \boldsymbol{M}_n \\ 0 & \boldsymbol{M}_v \end{bmatrix}$$

$$\boldsymbol{C} = \begin{bmatrix} 0 & 0 \\ 0 & \boldsymbol{C}_v \end{bmatrix}$$

$$\boldsymbol{K} = \begin{bmatrix} \boldsymbol{K}_b & \boldsymbol{K}_n \\ \boldsymbol{K}_m & \boldsymbol{K}_v \end{bmatrix}$$

$$\boldsymbol{F} = \begin{bmatrix} \boldsymbol{F}_b \\ 0 \end{bmatrix}$$

$$\boldsymbol{X}(t) = \left[u_1(t)\ u_2(t)\ \ldots\ u_n(t)\ \theta(t)\ y_v(t)\ y_1(t)\ y_2(t)\right]^T \tag{18}$$

Non-zero sub-matrices in the above equations are calculated as follows:

$$\left[\boldsymbol{M}_b\right]_{ij} = \rho A \int_0^L \varphi_i(x)\varphi_j(x)dx$$

$$\left[\boldsymbol{M}_n\right]_i = \left[0, a_{1,2}, a_{1,3}, a_{1,4}\right]$$

$$a_{1,2} = \frac{m_v}{b_1 + b_2}\left(b_1\varphi_i(x_2(t)) - b_2\varphi_i(x_1(t))\right)$$

$$a_{1,3} = -m_1\varphi_i(x_1(t))$$

$$a_{1,4} = -m_2\varphi_i(x_2(t))$$

$$\boldsymbol{M}_v = diag(I_v, m_v, m_1, m_2)$$

$$\boldsymbol{C}_v = \begin{bmatrix} c_1b_1^2 + c_2b_2^2 & c_1b_1 - c_2b_2 & -c_1b_1 & c_2b_2 \\ c_1b_1 - c_2b_2 & c_1 + c_2 & -c_1 & -c_2 \\ -c_1b_1 & -c_1 & c_1 & 0 \\ c_2b_2 & -c_2 & 0 & c_2 \end{bmatrix}$$

$$\left[\boldsymbol{K}_b\right]_{ij} = EI\int_0^L \varphi_i''(x)\varphi_j''(x)dx + k_{1s}\varphi_i(x_1(t))\varphi_j(x_1(t)) + k_{2s}\varphi_i(x_2(t))\varphi_j(x_2(t))$$

$$\left[\boldsymbol{K}_n\right]_i = \left[0, 0, -k_1\varphi_i(x_1(t)), -k_2\varphi_i(x_2(t))\right]$$

$$\left[\boldsymbol{K}_m\right]_j = \left[0, 0, -k_{1s}\varphi_j(x_1(t)), -k_{2s}\varphi_j(x_2(t))\right]^T$$

$$\boldsymbol{K}_v = \begin{bmatrix} k_1b_1^2 + k_2b_2^2 & k_1b_1 - k_2b_2 & -k_1b_1 & k_2b_2 \\ k_1b_1 - k_2b_2 & k_1 + k_2 & -k_1 & -k_2 \\ -k_1b_1 & -k_1 & k_1 + k_{1s} & 0 \\ k_2b_2 & -k_2 & 0 & k_2 + k_{2s} \end{bmatrix}$$

$$\left[\boldsymbol{F}_b\right]_j = \left(m_1 + \frac{b_2}{b_1 + b_2}m_v\right)g\varphi_j(x_1(t)) + \left(m_2 + \frac{b_1}{b_1 + b_2}m_v\right)g\varphi_j(x_2(t)) \tag{19}$$

The differential equations governing the cracked beam are the same as the relationships obtained in the case of a healthy beam, except that in this case, the mode shapes and the natural frequencies of the cracked beam obtained through the matrix method [32] are replaced with the mode shapes and the natural frequencies of the healthy beam in the above relations. This method can also be used for beams with multiple cracks.

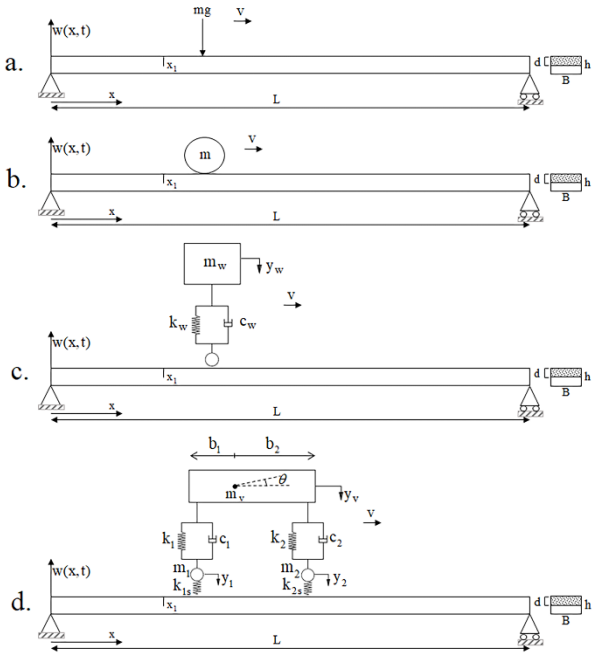

Fig. 1: An image of different moving forces;
(a. Moving load, b. Moving mass, c. Moving oscillator, d. Moving system.)

3. Solving the equations

In this study, a numerical method based on the concept of state space has been used to find the amplitude of the deformation of the beam under moving load in the time domain and to solve its motion equation. According to this method, Eq. (3) is rewritten as follows:

$$\dot{\boldsymbol{Q}}(t) = \boldsymbol{A}(t)\boldsymbol{Q}(t) + \boldsymbol{F}(t) \tag{20}$$

where

$$\boldsymbol{Q}(t) = \begin{bmatrix} \boldsymbol{u}(t) \\ \dot{\boldsymbol{u}}(t) \end{bmatrix}_{k\times 1},$$

$$\boldsymbol{A}(t) = \begin{bmatrix} 0 & \boldsymbol{I} \\ -\boldsymbol{M}^{-1}\boldsymbol{K} & -\boldsymbol{M}^{-1}\boldsymbol{C} \end{bmatrix}_{k\times k},$$

$$\boldsymbol{F}(t) = \begin{bmatrix} 0 \\ \boldsymbol{M}^{-1}\boldsymbol{F} \end{bmatrix}_{k\times 1} \tag{21}$$

In the above relations, *k* is as follows:

[DOR: 20.1001.1.23454296.2022.6.4.2.9]
[DOI: 10.52547/nmce.6.4.38]

$$k = \begin{cases} 2n & ; \text{ for moving force \& moving mass} \\ 2n+2 & ; \text{ for moving oscillator} \\ 2n+8 & ; \text{ for moving system} \end{cases}$$

Moreover, n is the number of considered mode shapes. Equation (20) is assumed to be as follows:

$$\boldsymbol{Q}(t_{k+1}) = \bar{\boldsymbol{A}}(t_k)\boldsymbol{Q}(t_k) + \bar{\boldsymbol{F}}(t_k) \quad (22)$$

So that:

$$\bar{\boldsymbol{A}}(t_k) \cong e^{A(t_k)\Delta(t_k)}, \bar{\boldsymbol{F}}(t_k) \cong [\bar{\boldsymbol{A}}(t_k) - \boldsymbol{I}]\boldsymbol{A}^{-1}(t_k)\boldsymbol{F}(t_k) \quad (23)$$

In these equations $\Delta(t_k) = t_{k+1} - t_k$ is assumed a small time step. Finally, by numerically solving Eq. (22), the value of $\boldsymbol{Q}(t)$ at any moment could be calculated. Finding it will lead to the determination of $\boldsymbol{u}(t)$.

4. Verifying example

In this section, an example is used to verify the accuracy of the theoretical relationships presented in the previous section to calculate the displacement responses. This example studies the situation in which a moving system passes over a simple-span simply supported beam, and the results of it are reported in another research [5]. The assumed beam has a length of L = 30 m, a moment of inertia of I = $0.2\ m^4$, q modulus of elasticity of $E = 27.5\ GPa$, and a mass per unit length of $\bar{m} = 2000\ kg/m$. A moving system with the lumped mass $M_v = 2500\ kg$, the moment of inertia around the center of mass $I_v = 2300\ kg.m^2$, axial distances $b_1 = 1.3\ m$ and $b_2 = 1.7\ m$, springs with stiffness $k_1 = 180\ KN/m$ and $k_2 = 230\ KN/m$ with speed $v = 10\ m/s$ passes over the beam. The contact surface between the beam and the wheels is assumed to be without friction, and the moving system is considered without damping. The response of the vertical displacement of the midpoint of the beam span for the first five modes with time intervals of $\Delta t = 0.001\ sec$ is shown in Fig. 2.

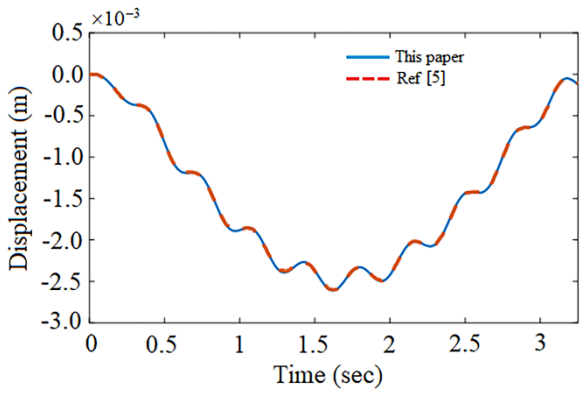

Fig. 2: Time history responses of displacement at the mid-span

As it can be seen, there is a very good agreement between the results obtained from the theoretical relationships of this research and the results reported from the Reference [5].

5. Numerical example

In this section, some numerical examples are used to review the studies. In all these examples, the properties of the beams are the same as a uniform beam with the length $L=25m$, cross-sectional dimensions $B=30\ cm$ and $h=60\ cm$, modulus of elasticity $E=2.1\times10^{11}\ N/m^2$, volumetric mass $\rho=7800\ kg/m^3$, and a crack at a distance of $x_1=0.3L$ from the left support. The specifications of the moving forces are as shown in Table 1. The first six modes are used to solve the equations and the time interval is also equal to $0.001\ sec$. The normalized speed, mass, and displacement parameters have been used to simplify the calculations. The normalized velocity parameter is defined by $V_n = v/v'$. In this equation, the base velocity is $v' = \frac{\pi}{L}\sqrt{\frac{EI}{\rho A}}$. The normalized load magnitude parameter is $M_n = M/M_b$, where M_b is the mass of the beam.

Table 1: The properties of moving forces

Type	parameter	Assumed measure
Moving load	$m\ (kg)$	7020
Moving mass	$m\ (kg)$	7020
Moving oscillator	$m\ (kg)$	7020
	$c\ (Ns/m)$	1
	$k\ (N/m)$	725.76
Moving system	$m_v\ (kg)$	7000
	$m_1, m_2\ (kg)$	10
	$c_1, c_2\ (Ns/m)$	1
	$k_1, k_2\ (N/m)$	725.76
	$k_{1s}, k_{2s}\ (N/m)$	725.76
	$b_1, b_2\ (m)$	0.5

$W_n = \frac{|W_{dyn,max}|}{|W_{sta,max}|}$ is also the normalized displacement parameter, where $W_{dyn,max}$ is the maximum displacement response of the beam when vibrating and $W_{sta,max}$ is the maximum static displacement response obtained from the following equation:

$$|W_{sta,max}| = \frac{mgL^3}{48\,EI}$$

The values of each of these normalized parameters can be seen in Table 2. The purpose of the following examples is to determine the effect of each of the factors of crack depth ratio ($D_c = \frac{d}{h}$), the type of moving force, wheel distance of the moving system, load magnitude of moving force, and

[DOR: 20.1001.1.23454296.2022.6.4.2.9]
[DOI: 10.52547/nmce.6.4.38]

crack position on the maximum displacement response of the beam at the midpoint.

Table 2: Assumed values of the normalized parameters

Parameter	values				
V_n	0.025	0.05	0.075	…	1
M_n	0.05	0.1	0.15	0.2	

In the first step of this stage, the beam is examined under each type of moving force (moving load, moving mass, moving oscillator, and moving system) with $M_n = 0.15$. Figure 3 shows the maximum normalized beam displacement response due to changes in the speed of various moving force types.

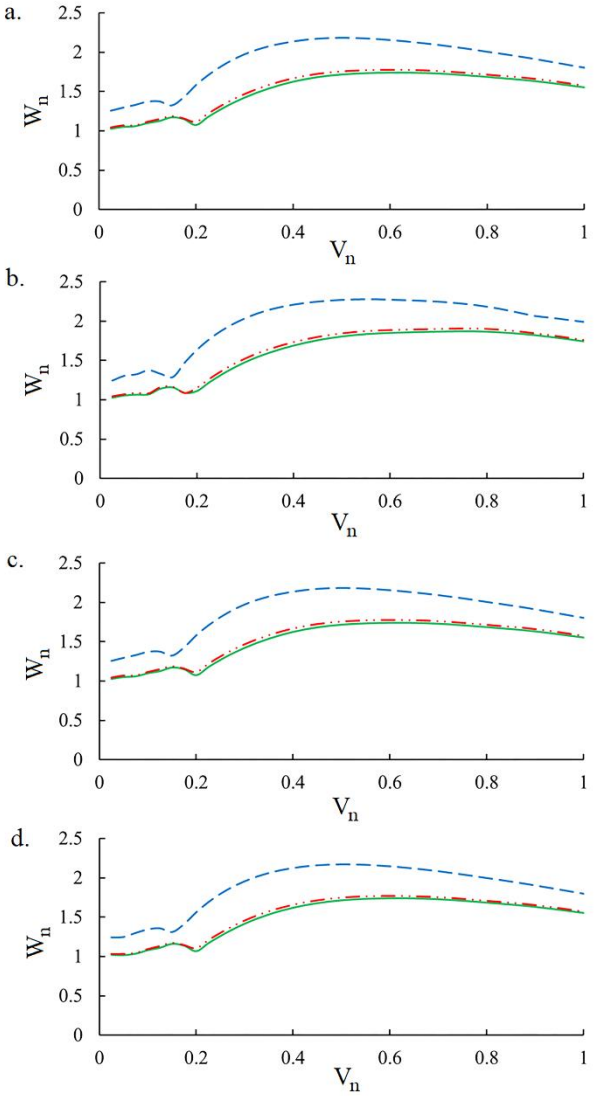

Fig. 3: The effect of normalized velocity on the normalized displacement of the cracked beam at mid-span with different crack depth ratios under a moving force (a. Moving load; b. Moving mass; c. Moving oscillator; d. Moving system); $D_c=0.1$ ——, $D_c=0.2$ – · – · –, $D_c=0.5$ – – –.

In this figure, the spectra are plotted for different crack depth ratios. As it can be seen, the deeper the crack depth in the beam section is, the greater displacement of the beam under the passage of various moving loads will be created, and the corresponding spectra will have a higher position. This is true for all mentioned loading conditions such as moving load, moving mass, moving oscillator, and moving system. For example, by plotting the beam displacement response separately for velocities $V_n = 0.1$, 0.6 and in conditions where the crack depth ratio increases from $D_c = 0.1$ to $D_c = 0.9$, Fig. 4 is obtained. Figure 4-a for $V_n = 0.1$, $M_n = 0.15$, and also Fig. 4-b for $V_n = 0.6$, $M_n=0.15$ show that the displacement response will increase with increasing crack depth ratio in the cross-section of the beam. In these figures, it can be seen that the beam under moving mass has a different response from other moving force states (moving load, moving oscillator, and moving system).

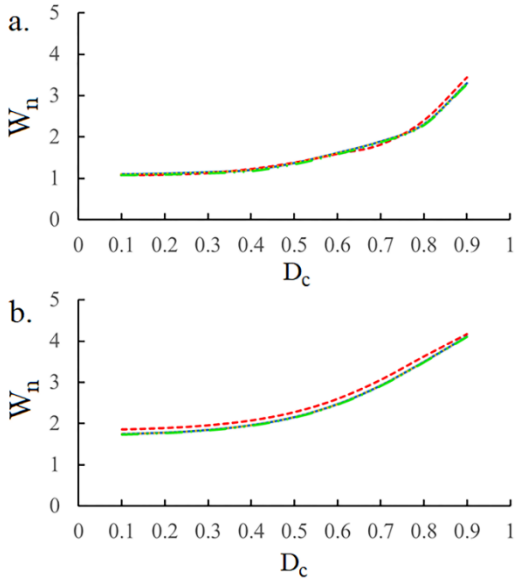

Fig. 4: The effect of crack depth ratio on the normalized deflection of the cracked beam at mid-span (a. $V_n=0.1$; b. $V_n=0.6$) and $M_n=0.15$; Moving load ——, Moving mass – – –, Moving oscillator ·····, Moving system – · – · –.

To compare the efficiency of the beam under different types of moving force, Fig. 5 investigates the spectra of the velocity-maximum response of the beam displacement under a different type of moving force (moving load, moving mass, moving oscillator, and moving system) with $M_n = 0.15$. This figure illustrates that under the same conditions, the beam fluctuated by the moving load, the moving oscillator, and the moving system has very similar responses, but with the passage of the moving mass over it, the displacement responses will generally have larger values.

It is also observed that, in general, as the normalized velocity increases, the difference between the moving mass spectra

[DOR: 20.1001.1.23454296.2022.6.4.2.9]
[DOI: 10.52547/nmce.6.4.38]

and other states increases. It is obvious that the reason for this deviation is the effect of inertia on the moving mass.

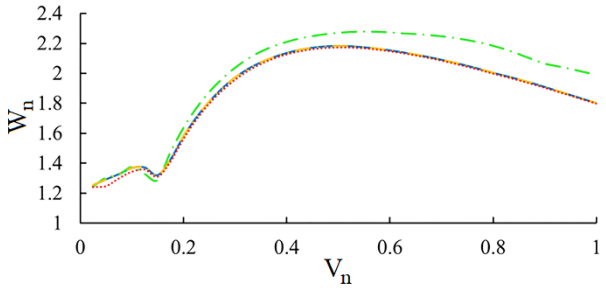

Fig. 5: The effect of moving load type velocity on the normalized displacement of the cracked beam at mid-span; Moving load ——— , Moving mass – · – · – , Moving oscillator – ·· – ··, Moving system ····· .

Now let us study the effect of the change in the distance between the wheels of the moving system in Fig. 6. As it can be seen, by increasing the distance of the wheels of the moving system, the displacement response of the beam decreases slightly but still does not have a significant effect.

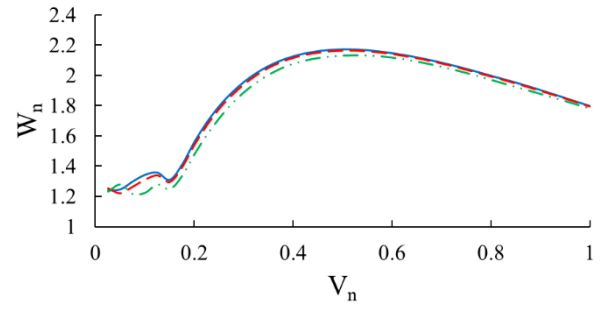

Fig. 6: The effect of the moving system wheel's distance on the normalized displacement of the cracked beam at mid-span; distance=1*m* ———, distance=1.5*m* – – –, distance=2.5*m* – ·· – ··.

In the next step, the spectra of changes in the magnitude of each moving force type on the maximum displacement response of the mid-span are checked (Fig. 7). The crack depth ratio is assumed to be $D_c = 0.5h$, and the normalized moving load velocity is $V_n = 0.4$.

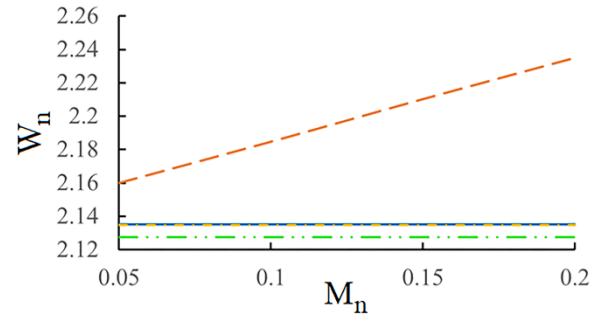

Fig. 7: The effect of moving load magnitude changes on the normalized displacement of cracked beam at mid-span; Moving load ———, Moving mass – – – , Moving oscillator – · – · – , Moving system – ·· – ·· .

Figure 7 represents that the beam displacement response under moving load, moving oscillator, and the moving system remains constant due to mass changes and does not change at all. While for the sake of increasing in load magnitude of the moving mass, the response of the beam displacement increases linearly.

On the other hand, to distinguish the effect of the crack location in the beam span on the maximum displacement response of it under each type of loading, it is assumed that there is a crack with a depth ratio of $D_c = 0.5h$ in the distance of x/L from the left support (Fig. 8). The normalized velocity of the moving force when passing over the beam and the normalized mass of it is considered to be $V_n = 0.6$ and $M_n = 0.15$. This figure denotes that the closer the crack location is to the center of the beam, the greater the maximum displacement response it will have. It is again observed that under the same situations, the dynamic responses of the beam under moving mass have a greater value than other moving force conditions.

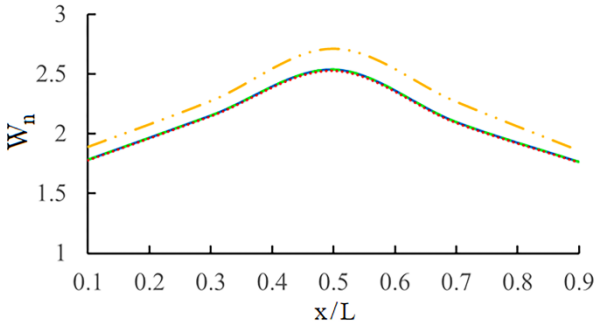

Fig. 8: The effect of crack location on the displacement of the cracked beam at mid-span; Moving load ———, Moving mass – ·· – ··, Moving oscillator – – –, Moving system ····· .

6. Conclusions

In this paper, the dynamic behavior of a cracked beam under moving forces such as moving load, moving mass, moving oscillator, and four degrees of freedom moving system was studied. First, a hinged beam was assumed in the form of a numerical example. Then the maximum response of its vibrations was extracted under the considered moving loads. At each step, the effect of parameters such as speed, load magnitude, crack depth ratio and location, and also the effect of the distance between the wheels of the moving system on the maximum deformation response of the midpoint of the beam was investigated. These responses were plotted in the form of spectra and compared with each other. By comparing these spectra, the following results were obtained:

- By increasing the crack depth ratio, the displacement response of the cracked beam under each type of the moving force becomes greater, and the related velocity-displacement

[DOR: 20.1001.1.23454296.2022.6.4.2.9]
[DOI: 10.52547/nmce.6.4.38]

spectra are in a higher position. This becomes clearer at higher speeds.

- By increasing the crack depth ratio at a constant speed, the displacement response increases.
- Increasing the distance of the wheels of the moving system decreases the displacement response of the beam slightly but still does not have a significant effect
- Increasing the load magnitude of the moving load, the moving oscillator, and the moving system did not change the beam displacement responses. However, by increasing it in the moving mass case, the beam displacement response increases linearly.
- If the location of the crack is closer to the middle of the beam, the response of the cracked beam will be higher. Conversely, if the crack is closer to the supports, the displacement response will be lower.
- Overall, by comparing the response spectra of the cracked beam displacement under different types of moving force, it is observed that its displacement response under moving load, moving oscillator, and moving system have very close values. Nonetheless, the displacement response under moving mass had higher values due to the inertial effect, so its spectra are in a higher position.

References

[1] Ostachowicz, W. and M. Krawczuk, *Analysis of the effect of cracks on the natural frequencies of a cantilever beam.* Journal of sound and vibration, 1991. **150**(2): p. 191-201.

[2] Pesterev, A., et al., *Response of elastic continuum carrying multiple moving oscillators.* Journal of engineering mechanics, 2001. **127**(3): p. 260-265.

[3] Muscolino, G., A. Palmeri, and A. Sofi, *Absolute versus relative formulations of the moving oscillator problem.* International Journal of Solids and Structures, 2009. **46**(5): p. 1085-1094.

[4] Van Do, V.N., T.H. Ong, and C.H. Thai, *Dynamic responses of Euler–Bernoulli beam subjected to moving vehicles using isogeometric approach.* Applied Mathematical Modelling, 2017. **51**: p. 405-428.

[5] Yang, Y., et al., *Two-axle test vehicle for bridges: Theory and applications.* International Journal of Mechanical Sciences, 2019. **152**: p. 51-62.

[6] Şimşek, M., *Dynamic analysis of an embedded microbeam carrying a moving microparticle based on the modified couple stress theory.* International Journal of Engineering Science, 2010. **48**(12): p. 1721-1732.

[7] Arani, A.G., M. Roudbari, and S. Amir, *Nonlocal vibration of SWBNNT embedded in bundle of CNTs under a moving nanoparticle.* Physica B: Condensed Matter, 2012. **407**(17): p. 3646-3653.

[8] Lee, H. and T. Ng, *Dynamic response of a cracked beam subject to a moving load.* Acta Mechanica, 1994. **106**(3): p. 221-230.

[9] Law, S. and X. Zhu, *Dynamic behavior of damaged concrete bridge structures under moving vehicular loads.* Engineering Structures, 2004. **26**(9): p. 1279-1293.

[10] Mahmoud, M. and M. Abou Zaid, *Dynamic response of a beam with a crack subject to a moving mass.* Journal of Sound and Vibration, 2002. **256**(4): p. 591-603.

[11] Nikkhoo, A., F. Rofooei, and M. Shadnam, *Dynamic behavior and modal control of beams under moving mass.* Journal of Sound and Vibration, 2007. **306**(3-5): p. 712-724.

[12] Kiani, K., A. Nikkhoo, and B. Mehri, *Assessing dynamic response of multispan viscoelastic thin beams under a moving mass via generalized moving least square method.* Acta Mechanica Sinica, 2010. **26**(5): p. 721-733.

[13] Kiani, K. and B. Mehri, *Assessment of nanotube structures under a moving nanoparticle using nonlocal beam theories.* Journal of Sound and Vibration, 2010. **329**(11): p. 2241-2264.

[14] Kiani, K. and Q. Wang, *On the interaction of a single-walled carbon nanotube with a moving nanoparticle using nonlocal Rayleigh, Timoshenko, and higher-order beam theories.* European Journal of Mechanics-A/Solids, 2012. **31**(1): p. 179-202.

[15] Kiani, K., *Nanoparticle delivery via stocky single-walled carbon nanotubes: a nonlinear-nonlocal continuum-based scrutiny.* Composite Structures, 2014. **116**: p. 254-272.

[16] Ghorbanpour Arani, A., M.A. Roudbari, and K. Kiani, *Vibration of double-walled carbon nanotubes coupled by temperature-dependent medium under a moving nanoparticle with multi physical fields.* Mechanics of Advanced Materials and Structures, 2016. **23**(3): p. 281-291.

[17] Thatoi, D., et al. *Analysis of the dynamic response of a cracked beam structure*. in *Applied mechanics and materials*. 2012. Trans Tech Publ.

[18] Pala, Y. and M. Reis, *Dynamic response of a cracked beam under a moving mass load.* Journal of Engineering Mechanics, 2013. **139**(9): p. 1229-1238.

[19] Jena, S.P. and D.R. Parhi, *Dynamic response and analysis of cracked beam subjected to transit mass.* International Journal of Dynamics and Control, 2018. **6**(3): p. 961-972.

[20] Cicirello, A., *On the response bounds of damaged Euler–Bernoulli beams with switching cracks under moving masses.* International Journal of Solids and Structures, 2019. **172**: p. 70-83.

[21] Al Rjoub, Y.S. and A.G. Hamad. *Forced vibration of axially-loaded, multi-cracked Euler-Bernoulli and Timoshenko beams*. in *Structures*. 2020. Elsevier.

[22] Nikkhoo, A. and M. Sharifinejad, *The impact of a crack existence on the inertial effects of moving forces in thin beams.* Mechanics Research Communications, 2020. **107**: p. 103562.

[23] Nikkhoo, A. and F.R. Rofooei, *Parametric study of the dynamic response of thin rectangular plates traversed by a moving mass.* Acta Mechanica, 2012. **223**(1): p. 15-27.

[DOR: 20.1001.1.23454296.2022.6.4.2.9]

[DOI: 10.52547/nmce.6.4.38]

[24] Nikkhoo, A., *Investigating the behavior of smart thin beams with piezoelectric actuators under dynamic loads.* Mechanical Systems and Signal Processing, 2014. **45**(2): p. 513-530.

[25] Nikkhoo, A., S. Zolfaghari, and K. Kiani, *A simplified-nonlocal model for transverse vibration of nanotubes acted upon*

by a moving nanoparticle. Journal of the Brazilian Society of Mechanical Sciences and Engineering, 2017. **39**(12): p. 4929-4941.

[26] Kiani, K., A. Nikkhoo, and B. Mehri, *Prediction capabilities of classical and shear deformable beam models excited by a moving mass.* Journal of Sound and Vibration, 2009. **320**(3): p. 632-648.

[27] Maghsoodi, A., A. Ghadami, and H.R. Mirdamadi, *Multiple-crack damage detection in multi-step beams by a novel local flexibility-based damage index.* Journal of sound and vibration, 2013. **332**(2): p. 294-305.

[28] Moezi, S.A., E. Zakeri, and A. Zare, *A generally modified cuckoo optimization algorithm for crack detection in cantilever Euler-Bernoulli beams.* Precision Engineering, 2018. **52**: p. 227-241.

[29] Attar, M., *A transfer matrix method for free vibration analysis and crack identification of stepped beams with multiple edge cracks and different boundary conditions.* International Journal of Mechanical Sciences, 2012. **57**(1): p. 19-33.

[30] Al Rjoub, Y.S. and A.G. Hamad, *Free Vibration of Axially Loaded Multi-Cracked Beams Using the Transfer Matrix Method.* International Journal of Acoustics & Vibration, 2019. **24**(1).

[31] Hudson, D.E., *Dynamics of structures: Theory and applications to earthquake engineering, by Anil K. Chopra, Prentice-Hall, Englewood Cliffs, NJ, 1995. No. of pages: xxviii+ 761, ISBN 0-13-855214-2.* 1995, John Wiley & Sons, Ltd New York.

[32] Lin, H.P., S.C. CHANG, and J.-D. Wu, *Beam vibrations with an arbitrary number of cracks.* Journal of Sound and Vibration, 2002. **258**(5): p. 987-999

[DOR: 20.1001.1.23454296.2022.6.4.2.9]

[DOI: 10.52547/nmce.6.4.38]